Phases of Ca from first principles

2009 J. Phys.: Condens. Matter 21 435403

(http://iopscience.iop.org/0953-8984/21/43/435403)

J. Phys.: Condens. Matter **21** (2009) 435403 (8pp) doi:10.1088/0953-8984/21/43/435403

Phases of Ca from first principles

S L Qiu[1] **and P M Marcus**[2]

[1] Department of Physics, Florida Atlantic University, Boca Raton, FL 33431-0991, USA
[2] IBM Research Division, T J Watson Research Center, Yorktown Heights, NY 10598, USA

Received 29 June 2009
Published 8 October 2009
Online at stacks.iop.org/JPhysCM/21/435403

Abstract

Structures and properties of many of the phases of Ca under pressure are calculated from first principles by a systematic procedure that minimizes total energy E with respect to structure under the constraint of constant volume V. The minima of E are followed on successive sweeps of lattice parameters for 11 of 14 Bravais symmetries for one-atom-per-cell structures. The structures include the four orthorhombic phases. Also included are the hexagonal close-packed and cubic diamond phases with two atoms per primitive cell. No uniquely orthorhombic phases are found; all one-atom orthorhombic phases over a mega-bar pressure range are identical to higher-symmetry phases. The simple cubic phase is shown to be stable where it is the ground state. The number of distinct one-atom phases reduces to five plus the two two-atom phases. For each of these phases the Gibbs free energy at pressure p, $G(p)$, is calculated for a non-vibrating lattice; the functions $G(p)$ give the ground state at each p, the relative stabilities of all phases and the thermodynamic phase transition pressures for all phase transitions over a several-megabar range.

1. Introduction

An infinite periodic crystal under pressure can have many equilibrium states or phases, which change with pressure. Stable phases have local stability in that the stresses produced by small deformations tend to return the phase to the equilibrium state. At any pressure p the phase with the lowest Gibbs free energy G is the ground-state phase and is always stable. The value of G changes with p for each phase, so the ground-state phase can change with p. At each p there is a hierarchy of phases with higher G values than the ground state; these phases have varying degrees of local stability and are designated metastable [1].

The purpose of this paper is to describe and apply a systematic first-principles procedure which we have applied previously [1–5] to find the structures and properties of the phases of elements as functions of p, including the Gibbs free energy $G(p)$. For Ca more phases are studied than we studied in previous elements. However we limit the systems studied here to non-vibrating infinite crystals of Ca with one atom per primitive cell, and two two-atoms-per-cell phases in which the position of the second atom is locked in by symmetry. The difficulty of the calculation increases as the symmetry is lowered. The application here is to all the one-atom phases of Ca with 11 symmetries of the 14 possible Bravais symmetries, including the four orthorhombic symmetries.

We exhibit for each phase the equilibrium line [4] plotted in structure space, which provides a complete description of the changes in structure as p changes. Quantitative values of p appear along the line, as well as ranges of p where the phase is unstable; in these ranges the phase is still in an equilibrium state (the gradient of G vanishes), but G has a saddle point rather than a minimum. The designation of a phase as unstable is confined here to one-atom-per-cell phases (one-atom phases for short); in later developments the designation unstable will also be applied to two-atom cells. The comprehensive character of our procedure ensures that all one-atom phases in the range of pressures and for the 11 symmetries studied are found; the pressure goes up to 1–2 Mbar. Several new high-pressure phases are found—a bct phase at 1.4 Mbar; an hcp phase at 2.1 Mbar.

Extension of the procedure for finding one-atom phases to monoclinic and triclinic symmetries is straightforward, as is extension to two-atom cells. We can then determine if there are one-atom phases that have these symmetries, but are different from higher-symmetry phases. Two-atom phases with these symmetries are more likely, as is the case for orthorhombic symmetries. Extension of the procedure to more than two-atom cells appears possible with increased computation.

The results are summarized in a plot of ΔG versus p, where ΔG is the difference of the G of each phase from a reference phase. These $\Delta G(p)$ functions give directly the ground-state phase, the relative stabilities of the metastable phases, and the p values at which thermodynamic phase transitions are favored, and from the first and second p

Table 1. Phases of Ca studied in this work; the short symbol, full name and degrees of freedom for each phase.

Short symbol	Phase name	Degrees of freedom
sc	simple cubic	1
fcc	face-centered cubic	1
bcc	body-centered cubic	1
cd	cubic diamond	1
st	simple tetragonal	2
bct	body-centered tetragonal	2
rh	rhombohedral	2
sh	simple hexagonal	2
hcp	hexagonal close packed	2
orth1	simple orthorhombic	3
orth2	body-centered orthorhombic	3
orth3	base-centered orthorhombic	3
orth4	face-centered orthorhombic	3

derivatives of ΔG we obtain respectively the difference in the volume V and the difference in V/B for the phase from the reference phase values, where B is the bulk modulus. In addition we make a test for absolute stability of the one-atom-per-cell phases at each p.

Section 2 describes the successive-sweep procedure used to find phases.

Section 3 gives results of calculations on the 13 phases of Ca listed in table 1.

Section 4 discusses the limitations of the procedure for finding phases, some interesting features of the results on the 13 phases studied here, and the value of the $\Delta G(p)$ results.

2. Computational details

Our procedures [1–5] find crystal phases, their structures, equilibrium lines (eql), stabilities, and pressures of inter-phase transitions (thermodynamic coexistence) in five stages of calculation. The procedure finds and follows the minima of E at constant V as the lattice parameters are successively swept. If there are N parameters, then $N-1$ sweeps are made under the constraint of constant V.

The first stage finds states of a particular symmetry corresponding to minima of the internal energy E at constant volume V. These minima would be equilibrium states for cubic symmetry, but not for lower symmetries. For finding and characterizing the phases of a two-parameter structure such as bct, hcp, sh, rh and st we look for minima of E at constant V as a function of one parameter, e.g., c/a for bct, where $a = b \neq c$; at each minimum in $E_V(c/a)$ no further minimization is needed to find a phase since V and c/a fix the structure. There may be several minima on each $E_V(c/a)$ curve and each minimum corresponds directly to a phase. The energies at these minima are denoted $E^{\rm ph}(V)$, where ph refers to a particular phase. Repetition of the c/a sweep at V_i gives $E^{\rm ph}(V_i)$, $i = 1$–n, where V_i becomes small enough to cover the pressure range of interest.

Another example of the treatment of a two-parameter structure is given by rh phases; we calculate $E_V(\alpha)$ at constant volume $V_i, i = 1$–n, covering the pressure range of interest, where α is the structure angle. This rhombohedral sweep varies

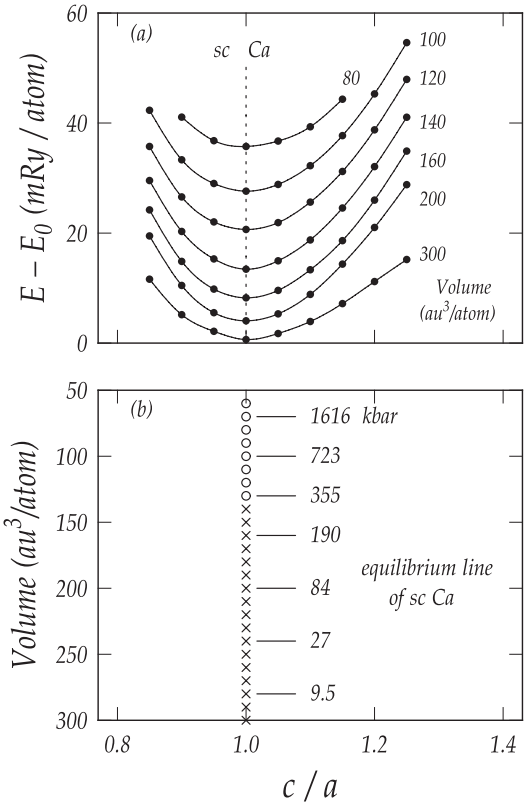

Figure 1. (a) Total internal energy as a function of c/a (called $E_V(c/a)$ curves) of sc phase of Ca at selected volumes. The reference E_0 is the total energy of sc Ca at $V = 300$ au^3/atom. For clarity the $E_V(c/a)$ curves at volumes from 200 to 80 au^3/atom are shifted toward E_0 by 17, 48, 74, 115, 184 and 304 mRyd/atom respectively. The solid lines interpolate between the calculated points. (b) Equilibrium line of sc phase of Ca. The open circles denote stable states; the crosses denote unstable states. The pressure values shown in (b) are obtained from figure 8.

the α values of a one-atom rh unit cell, which is formed by lattice vectors $(\vec{a}, \vec{b}, \vec{c})$ with $a = b = c$ and angles $\alpha = \beta = \gamma$. The one-atom fcc primitive unit cell is a special case of the one-atom *rh* unit cell with $a = \frac{\sqrt{2}}{2}a_0, \alpha = \alpha^{\rm fcc} = 60°$, where a_0 is the lattice constant of the conventional cubic fcc cell. The one-atom bcc unit cell is another special case of the one-atom rh unit cell with $a = \frac{\sqrt{3}}{2}a_0, \alpha = \alpha^{\rm bcc} = 109.47°$, where a_0 is the lattice constant of the conventional bcc cell. The volume of the rh unit cell is given by

$$V = a^3(1-\cos\alpha)\sqrt{1+2\cos\alpha}. \qquad (1)$$

At each V_i and α the value of a is found from (1). The minima in $E(\alpha)$ give directly the equilibrium states, i.e., give the phases and give $E^{\rm ph}(V_i)$ at volume V_i, $i = 1$–n in rh structure.

If the structure has three parameters such as orthorhombic structure (V, a, b, with $c = V/ab$) an additional minimization of E with respect to a second lattice parameter is needed; i.e., to find the values of $E^{\rm ph}(V)$ at a given V two sweeps are needed. The first can be a b-sweep at one value of lattice parameter a, and at the given V. The minima of E from the b-sweep may be designated $E_{\rm m}$ at $b_{\rm m}$ for the chosen a.

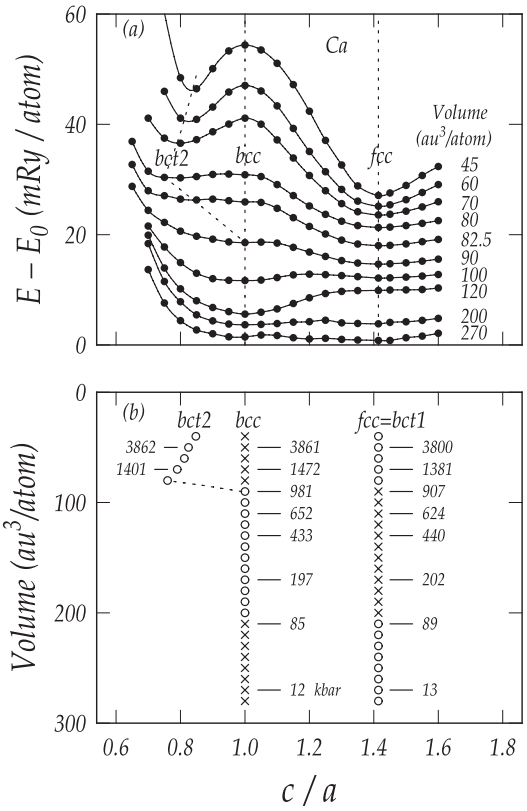

Figure 2. (*a*) $E_V(c/a)$ curves of bct Ca at selected volumes. The reference E_0 is the total energy of fcc Ca at $V = 270$ au^3/atom. For clarity the $E_V(c/a)$ curves at volumes from 200 to 45 au^3/atom are shifted toward E_0 by 21.5, 162, 245, 298, 364, 440, 548 and 886 mRyd/atom respectively. The vertical dashed lines indicate the bcc and fcc phases at $c/a = 1.00$ and 1.414 respectively. The c/a values of the bct phase vary with volume as indicated by the tilted dashed lines. The solid lines interpolate between the calculated points. (*b*) Equilibrium lines of the bct2, bcc and fcc = bct1 phases of Ca. The open circles denote stable states; the crosses denote unstable states. The pressure values shown in (*b*) are obtained from figure 8.

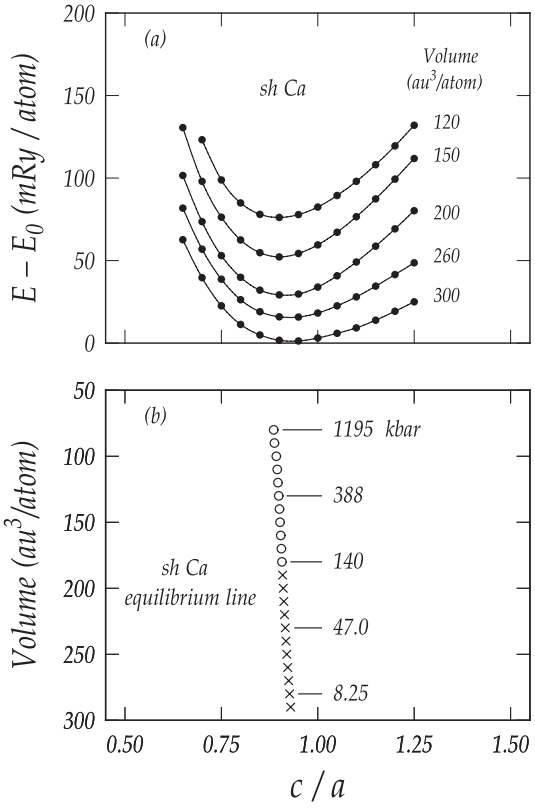

Figure 3. (*a*) $E_V(c/a)$ curves of simple hexagonal (sh) Ca at selected volumes. The reference E_0 is the total energy of sh Ca at $V = 300$ au^3/atom. For clarity the $E_V(c/a)$ curves at volumes from 260 to 120 au^3/atom are shifted toward E_0 by −12.4, −6.10, 25.0, 73.4 mRyd/atom respectively. The solid lines interpolate between the calculated points. (*b*) Equilibrium line of the sh phase of Ca. The open circles denote stable states; the crosses denote unstable states. The pressure values shown in (*b*) are obtained from figure 8.

Then we sweep the a values (and sweep b at each a) and find $E_m(a)$, $b_m(a)$; the minimum of $E_m(a)$ with respect to a gives E_{mm} and b_{mm} at a particular a, which can be called a_{mm}. Then E_{mm} gives the value of $E^{ph}(V)$ at the given V and a_{mm}, b_{mm}, $c_{mm} = V/(a_{mm}b_{mm})$ give the equilibrium structure parameters denoted ($a_{eq} = a_{mm}, b_{eq} = b_{mm}, c_{eq} = c_{mm}$), which provide a phase point in structure space. Repetition at a series of V values gives a series of $E^{ph}(V_i)$ $i = 1$–n and a series of phase points, where V_i should become small enough to cover the pressure range of interest.

In stage 2 the phase points (a_{eq}, b_{eq}, c_{eq}) as functions of V are used to find the equilibrium line of each phase. For structures with two lattice parameters the ratio c_{eq}/a_{eq} (call it c/a) versus V gives the equilibrium line of that phase, because a point ($c/a, V$) in structure space corresponds to one structure. When pressure p changes the crystal state moves along a one-dimensional continuum of states in structure space. For orthorhombic structures with three lattice parameters two equilibrium lines c_{eq}/a_{eq} and b_{eq}/a_{eq} versus V give the structure of one phase.

In stage 3 the values of $E^{ph}(V_i)$ are used to find the pressures as functions of V. These functions are different for different phases. The pressures are found from the energies $E^{ph}(V_i)$ at several adjacent V_i,

$$p^{ph}(V) = -dE^{ph}(V)/dV, \tag{2}$$

where the $p^{ph}(V)$ function is the equation of state (EOS) of just that phase.

In stage 4 the Gibbs free energy functions $G^{ph}(p)$ of the individual phases are found from the functions $E^{ph}(V)$ and $p^{ph}(V)$ (or the inverse function $V^{ph}(p)$) from stages 1 and 3,

$$G^{ph}(p) \equiv E^{ph}(V^{ph}(p)) + pV^{ph}(p). \tag{3}$$

Finally, in stage 5 we test each one-atom-per-cell phase for stability by our MNP (minimum path) program [2, 5]. The equilibrium states found from minima of E at constant V are not necessarily stable (a strain that changes V could decrease G); establishing stability of a state under pressure requires evaluation of G and proving that G is a minimum with respect to all possible small deformations around the equilibrium state. Proving a minimum of G is equivalent to showing the positive definiteness of the quadratic form in the

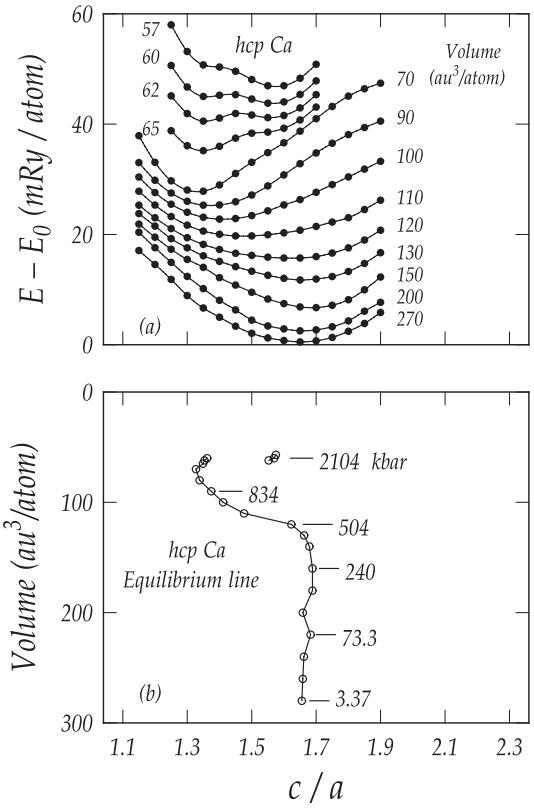

Figure 4. (*a*) $E_V(c/a)$ curves of hcp Ca at selected volumes. The reference E_0 is the total energy of hcp Ca at $V = 270$ au^3/atom. For clarity the $E_V(c/a)$ curves at volumes from 200 to 57 au^3/atom are shifted toward E_0 by 23.9, 82.5, 125, 153, 186, 226, 274, 417, 459, 491, 515 and 558 mRyd/atom respectively. (*b*) Equilibrium lines of the hcp phase of Ca. The pressure values shown in (*b*) are obtained from figure 8. In both (*a*) and (*b*) the solid lines interpolate between the calculated points.

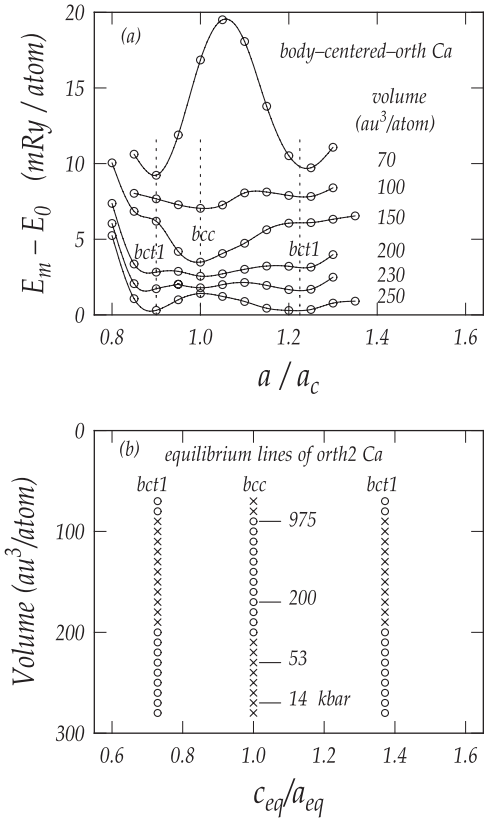

Figure 5. (*a*) The $E_m(a)$ curves at selected volumes for the body-centered-orthorhombic (orth2) phase of Ca. The reference E_0 is the total energy of orth2 Ca at $V = 250$ au^3/atom. For clarity the energy curves at volumes from 230 to 70 au^3/atom are shifted toward E_0 by 4.70, 19.5, 80.7, 247 and 452 mRyd/atom respectively. The solid lines interpolate between the calculated points. (*b*) Equilibrium lines for bct1 and bcc phases of orth2 Ca; the two bct1 lines have the same structure. The open circles denote stable states; the crosses denote unstable states. The pressure values shown in (*b*) are obtained from figure 8.

strains in the expression of δG:

$$\frac{\delta G}{V_0} \equiv \frac{G - G_0}{V_0} = \frac{1}{2}\sum_{i,j=1}^{6} c_{ij}\varepsilon_i\varepsilon_j. \qquad (4)$$

The second-order coefficients of δG are a set of elastic constants c_{ij}, $i, j = 1$–6. The MNP program evaluates $\delta G(p)$ for selected strains to determine the 21 elastic constants, which form a 6×6 symmetric matrix $c_{ij}(p)$ at each p; the program then finds the matrix eigenvalues (which the MNP program uses to seek out the minima of G at constant p, i.e., the phases). A negative eigenvalue means instability. The negative eigenvalue is a proof of the static instability of an equilibrium structure, i.e., a small strain exists that can lower the Gibbs free energy of the static structure.

The total internal energy is calculated using the WIEN2k package [6], which is an implementation of the full-potential augmented-plane-wave plus local orbital (APW + lo) method together with the Perdew–Burke–Ernzerhof generalized gradient approximation (PBE-GGA). The APW + lo method expands the Kohn–Sham orbitals in atomic-like orbitals inside the atomic spheres and plane waves in the interstitial region. A plane-wave cutoff $R_{\mathrm{MT}}K_{\max} = 7$, $R_{\mathrm{MT}} = 2.0$ au, $G_{\max} = 12$, mixer = 0.05 and 1000 k-points in the irreducible Brillouin zone were used in all the band calculations. The k-space integration was done by the modified tetrahedron method. Tests with larger basis sets and different Brillouin-zone samplings yielded only very small changes in the results. The convergence criterion on the energies is set at 1×10^{-3} mRyd (10^{-6} Ryd).

3. Results

The procedures described in section 2 have been applied to 13 phases of Ca, 11 of the 14 Bravais symmetries to phases with one atom per cell (sc, bct, bcc, fcc, st, sh, rh, orth1, orth2, orth3, orth4) and two two-atom-per-cell phases (hcp, cd). In figures 1–6 detailed results on eight phases are plotted (sc, bct, bcc, fcc, sh, hcp, orth2, orth3). The results for the other five phases (st, rh, cd, orth1, orth4) are straightforward with no unusual features and are not plotted. In figures 1–6 the upper plot is the energy as a function of a lattice parameter for several V values. For the one-degree-of-freedom structures (V) in (cd, sc, bcc, fcc) all values of E give phase points in structure

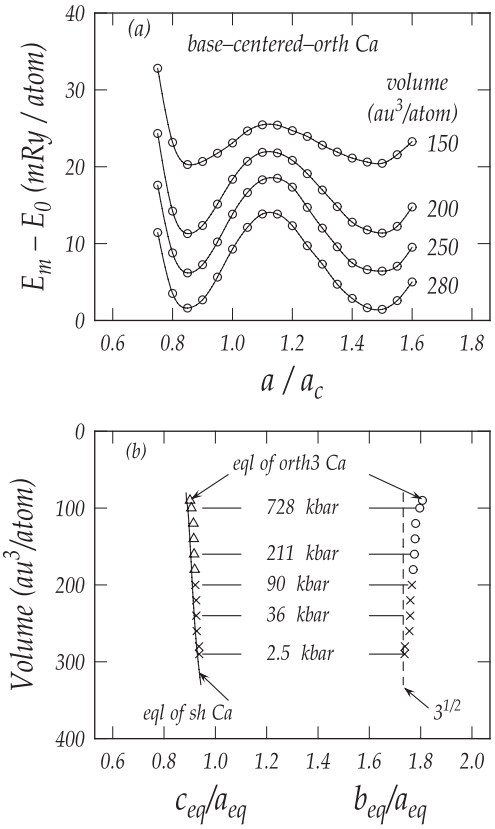

Figure 6. (a) The $E_{\rm m}(a)$ curves at selected volumes for the base-centered-orthorhombic (orth3) phase of Ca. The reference E_0 is the total energy of the orth3 Ca at $V = 280$ au^3/atom. For clarity the energy curves at volumes from 250 to 150 au^3/atom are shifted toward E_0 by -1.50, 11.5 and 57.0 mRyd/atom respectively. The solid lines interpolate between the calculated points. (b) Equilibrium lines of the orth3 phase of Ca. The open circles denote stable states; the crosses denote unstable states. The pressure values shown in (b) are obtained from figure 8. The solid line is the equilibrium line of the sh phase of Ca, which is the same as in figure 3(b). The overlapping of the equilibrium lines of the sh and the orth3 phases of Ca indicates that the equilibrium states of the orth3 phase have the sh structure. The dashed line corresponds to a constant value of $\sqrt{3}$.

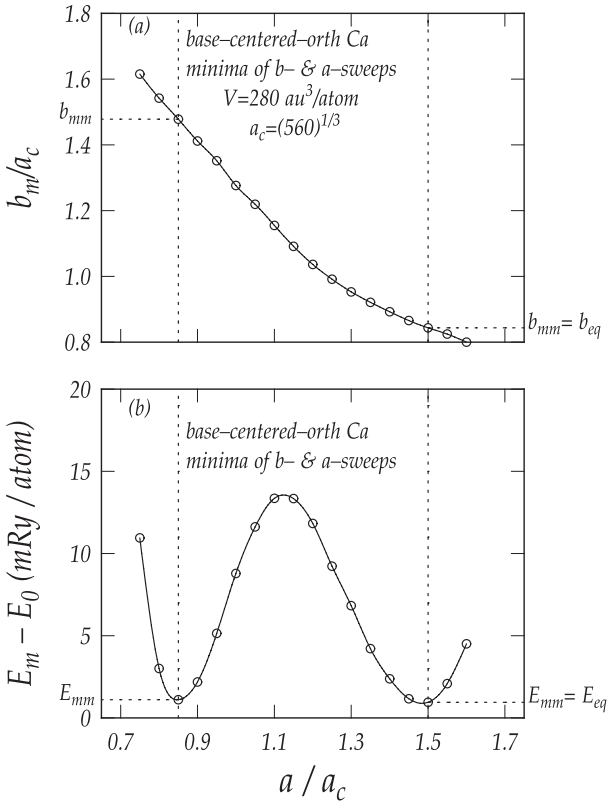

Figure 7. (a) Plot of the b values $b_{\rm m}(a)$ at the minimum of E at each a for the base-centered-orthorhombic (orth3) phase of Ca at $V = 280$ au^3/atom. (b) Total energy $E_{\rm m}(a)$ at each value of a plotted in (a) showing two equilibrium states at $a_{\rm eq} = 0.85a_c$ and $1.5a_c$ respectively which have the same energy, where $a_c = \sqrt[3]{V_{\rm cell}}$ and $V_{\rm cell}$ is volume per unit cell. This $E_{\rm m}(a)$ curve is the same as in figure 6(a) at $V = 280$ au^3/atom; $b_{\rm mm} = b_{\rm eq}$ and $E_{\rm mm} = E_{\rm eq}$ are values at the phase point. In both (a) and (b) the solid lines interpolate between the calculated points.

space; for the two-degrees-of-freedom structures (V, c/a) in (bct, sh, hcp) the minima of E as a function of the lattice parameters (e.g., c/a) give the phase points at each V; for the three-degrees-of-freedom structures (V, a, b) in (orth2, orth3) an additional step is needed. In the third case the energy values plotted are $E_{\rm m}(a)$, which are minima of E as functions of b at each a; this extra step is shown for orth3 in figure 7, where at each a minima of E as b varies give $E_{\rm m}(a)$ and $b_{\rm m}(a)$, which are plotted at one V. The phase points are then the minima of $E_{\rm m}(a)$, $E_{\rm mm} = E_{\rm eq}$ and the corresponding $b_{\rm mm} = b_{\rm eq}$.

In each of figures 1–6 the lower plot gives the equilibrium lines of the phase in a relevant structure space for that symmetry; along the equilibrium line two additional features appear: the stability or instability of points on the line is marked, which has been found as in stage 5 of section 2, and the pressures at several phase points are indicated. The pressures are found locally for each phase as described in stage 3 in section 2. The complete $p(V)$ functions for each phase are plotted in figure 8.

The p value and $E_{\rm eq}$ of each phase point are then used to find $G(p)$ as described in stage 4 in section 2. Figure 9 plots the free energy difference $\Delta G = G^{\rm ph} - G^{\rm fcc}$ as functions of p, where ph = fcc, bcc, bct, sc, rh, sh, st, cd, hcp, orth1, orth2, orth3, orth4, which gives an overall view of the phase transitions, making clear the relations of all the phases to each other.

We note some interesting features of the phase structures in figures 1–6. The equilibrium line of sc phase shown in figure 1(b) indicates that the sc phase of Ca is unstable below 355 kbar and stable from 355 kbar to at least 1616 kbar, corresponding to the last point on the $G^{\rm sc}$ curve in figure 9. Notice that the phase transition from fcc to sc takes place at $p = 355$ kbar where the sc phase becomes stable, then the sc phase becomes the ground state after the phase transition from bcc to sc at 420 kbar; these phase transitions can be seen in figure 9. Thus sc Ca is stable where it is the ground state and is observed experimentally. This result is in good agreement with [7, 8] but not [9], which finds that the sc phase of Ca is mechanically unstable from 0 to at least 1200 kbar. In figure 2 on the bct phase, which also contains the bcc and fcc = bct1 phases, the bcc phase is unstable at low p, becomes stable over a range of p, and then goes unstable again. At the second

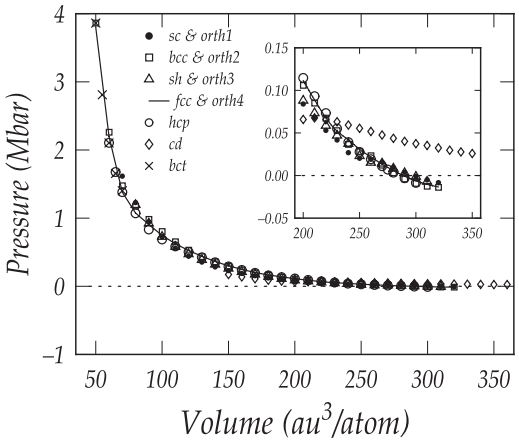

Figure 8. $p(V)$ curves for different phases of Ca, which are labeled by the following symbols: solid circles for sc, st and orth1 phases, open squares for bcc and orth2 phases, open triangles for sh and orth3 phases, solid line for fcc and orth4 phases, open circles for hcp phase, open diamonds for cd phase and crosses for bct phase. The crossing of the $p(V)$ curve with the dashed line ($p = 0$) shown in the inset gives the equilibrium volume: $V_0^{\rm fcc} = 288.5$ au^3/atom, $V_0^{\rm bcc} = 283.4$ au^3/atom, $V_0^{\rm hcp} = 285.0$ au^3/atom, $V_0^{\rm sc} = 295.6$ au^3/atom, $V_0^{\rm hex} = 296.4$ au^3/atom. There is no crossing for the $p(V)$ curve of the diamond phase of Ca.

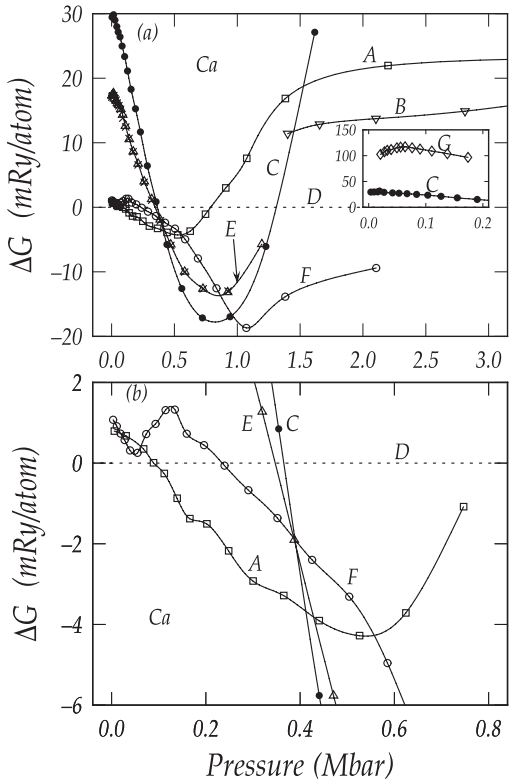

Figure 9. (a) Gibbs free energy difference curves between the fcc phase and the other phases of Ca, which are labeled by A, $G^{\rm bcc}$, $G^{\rm orth2\_bcc}$, $G^{\rm rh\_bcc}$; B, $G^{\rm bct2}$; C, $G^{\rm sc}$, $G^{\rm st}$, $G^{\rm orht1}$; D, $G^{\rm fcc}$, $G^{\rm bct1}$, $G^{\rm orth4}$, $G^{\rm rh\_fcc}$; E, $G^{\rm sh}$, $G^{\rm orth3}$; F, $G^{\rm hcp}$; G, $G^{\rm cd}$. Curve G is plotted in the inset along with curve C for a comparison of the energy scale. (b) Free energy difference curves A, C, D, E and F, plotted in an enlarged scale showing the phase transitions among the fcc, bcc, hcp, sh and sc phases of Ca. In both (a) and (b) the solid lines interpolate between the calculated points.

instability, $V = 90$ au^3/atom, a second bct phase (bct2) forms at $c/a < 1$. The fcc phase, which is bct in a two-atom cell, shows the inverse behavior, initially stable, then unstable, then stable again. The unstable ranges of the bcc and fcc phases cannot be deduced from curves in figure 2(a), but require a complete elastic analysis [2, 5] using the complete 6×6 matrix c_{ij}, $i, j = 1$–6, which is described in stage 5 in section 2.

The stability on the equilibrium line of the sh phase in figure 3(b) similarly requires the complete elastic analysis.

The hcp phase in figure 4 shows an abrupt deviation of c/a to smaller values under high pressure like the bcc phase in figure 2(a). However, we are unable at this time to find the stabilities along the equilibrium line, because the elastic analysis of two-atom cells is more complicated than for one-atom cells and is not yet built into our MNP program.

In figure 5 the orth2 structure shows three equilibrium lines. The structures are bct1, bcc and bct1 respectively, but the bct calculation in figure 2 shows only two equilibrium lines at low p—the bcc and fcc = bct1 lines. However, in figure 5 the equilibrium line at $c/a = 0.7$ is actually for the same structure as the one at $c/a = 1.4$ with the axes permuted ($b = c$), whereas the bct calculation in figure 2 forces $a = b$, hence does not find the 0.7 equilibrium line.

The correspondence of the orth3 phase to the sh phase is shown in figure 6(b), and is known, for example, from the behavior of the orthorhombic Imma phase of Si as it makes a transition to the sh phase [10]. The two equilibrium lines in figure 6(b) are actually the same orthorhombic structure with axes permuted.

The transition pressures obtained from figure 9 are listed in table 2 and compared to the experimental and theoretical results reported in the papers [7, 9, 11–17]. The energy differences $G^{\rm ph} - G^{\rm fcc}$ at $p = 0$ obtained from figure 9 are listed in table 3.

4. Discussion

This paper is a step toward the goal of finding all the phases of a given element over a pressure range of experimental interest. We have shown that with modest computation we can find phases with the successive-sweep procedure used here in which the unit cell has four degrees of freedom, such as monoclinic, or orthorhombic with one additional atom with one degree of freedom, tetragonal with an additional atom with two degrees of freedom, or cubic with an additional atom with three degrees of freedom. Here we study structures with one atom per cell having 11 of the possible 14 Bravais symmetries plus two two-atoms-per-primitive-cell structures, where the second atom is fixed by symmetry. However, the number of distinct structures is reduced to five one-atom-per-cell structures plus the two two-atoms-per-cell structures, because identical structures to high-symmetry crystals are found for lower-symmetry crystals that have special values of the structural parameters.

The four orthorhombic symmetries are studied comprehensively using one-atom cells over a pressure range up to

Table 2. Transition pressures (Mbar) for Ca.

References	fcc → bcc	bcc → sc	bcc → hcp	sc → unknown	sc → hcp
[11] (experiment)	0.195	0.32	—	0.42	—
This work (theory)	0.10	0.42	0.56	—	0.94
[7] (theory)	0.08	0.41	—	—	—
[9] (theory)	0.07	0.41	0.65	—	0.98
[12] (theory)	0.15	0.33	—	—	1.12
[13] [a] (theory)	0.07–0.21	—	0.80	—	—
[14] [b] (theory)	0.090–0.056	0.404–0.414	—	—	—
[15] (theory)	0.16 ± 0.05	—	—	—	—
[16] (theory)	0.0596	—	—	—	—
[17] [c] (theory)	0.09(?)	—	—	—	—

[a] The author states that the calculated pressure range for the semiconducting phase is found to be 7–21 GPa for Ca, within which the structural phase transition is calculated to occur.

[b] The first number does not, the second number does, include the zero-point energy calculated in the Debye approximation.

[c] The authors state that the fcc → bcc transition occurs at $V_T/V_{eq} \approx 0.6$, corresponding to ~ 0.2 Mbar; however, their figure 6 shows that $V_T/V_{eq} = 210/256.9 \simeq 0.82$, corresponding to ~ 0.09 Mbar.

Table 3. Energy differences $G^{ph} - G^{fcc} = E^{ph} - E^{fcc}$ of Ca at $p = 0$.

Phases of Ca	fcc	bct	bcc	hcp	sh & orth3	sc & st	cd
$G^{ph} - G^{fcc}$ at $p =$ 0 (mRyd/atom)	0.00	0.13	0.78	1.1	18	30	∼90 [a]

[a] This value is estimated from the slope of the first four points of curve G shown in the inset of figure 9(*a*). Notice that the EOS curve of cd phase does not cross the $p = 0$ line as shown in the inset of figure 8.

1–2 Mbar. An interesting result is that no uniquely orthorhombic phases with one atom per cell are found; all the phases found were the same as a higher-symmetry structure, which was produced by special relations among the orthorhombic lattice parameters.

Various physical and chemical properties of an element are directly described by the set of $\Delta G(p) \equiv G^{ph}(p) - G^{fcc}(p)$ curves, which give a characteristic 'fingerprint' and a phase diagram of an element. The $G(p)$ phase diagram shown in figure 9 is in good agreement with the phase diagrams reported in two recent papers for Ca [7, 9] for fcc, bcc, sc and hcp phases, which can be seen from the close values of the phase transition pressures among these phases listed in table 2. Our figure 9 differs from the phase diagrams in [7, 9] by including all the one-atom phases in 11 Bravais symmetries, but without the *Cmcm* and *Pnma* phases. From the $\Delta G(p)$ curves the ground-state phase at any p can be identified, the relative stability at p of every phase with respect to every other phase is shown, the p values of thermodynamically favored transitions (coexistence) between phases appear and the loss of stability that results in the vanishing of a phase appears. In addition, we have along the $G(p)$ curve $dG/dp = V, d^2G/dp^2 = V/B$, where B is the bulk modulus. For ΔG curves, the derivatives give the differences of V and V/B from the fcc phase values.

Additional properties of a phase along its equilibrium line that can be calculated and that we are studying are the following. (1) A quantitative measure of local stability is given by the change in G from the equilibrium G value at p to the lowest maximum of G in states at constant pressure around the equilibrium state. This measure of stability would identify especially stable metastable phases. Examples exist, and if the element can be brought into that phase the phase could be maintained for a long time. (2) The closest distance in structure space can be found between two phases whose $G(p)$ curves cross, indicating a thermodynamically favored transition between these phases. The smaller the distance, the more the phases will interact, e.g. affect the other's elastic properties.

Acknowledgments

The calculations were carried out using the computational resource Altix at the Center for High-Performance Computing at Florida Atlantic University funded by The National Science Foundation, under grant CNS-0521410. PMM thanks IBM for providing facilities as an Emeritus member of the Thomas J Watson Research Center.

References

[1] Qiu S L and Marcus P M 2008 *Eur. Phys. J.* B **66** 1
[2] Qiu S L and Marcus P M 2008 *J. Phys.: Condens. Matter* **20** 345233
[3] Qiu S L and Marcus P M 2008 *J. Phys.: Condens. Matter* **20** 275218
[4] Marcus P M and Qiu S L 2009 *J. Phys.: Condens. Matter* **21** 125404
[5] Marcus P M and Qiu S L 2009 *J. Phys.: Condens. Matter* **21** 115401
[6] Blaha P, Schwarz K, Madsen G K H, Kvasnicka G D and Luitz J 2001 *WIEN2k, An Augmented Plane Wave + Local Orbitals Program for Calculating Crystal Properties* Karlheinz Schwarz, Techn. Universität Wien, Austria

Blaha P, Schwarz K and Sorantin P 1990 *Comput. Phys. Commun.* **59** 399
[7] Arapan S, Mao H and Ahuja R 2008 *Proc. Natl Acad. Sci.* **105** 20627
[8] Yao Y S, Tse J S and Song Z 2008 *Phys. Rev.* B **78** 054506
[9] Teweldeberhan A M and Bonev S A 2008 *Phys. Rev.* B **78** 140101
[10] Lewis S P and Cohen M L 1993 *Phys. Rev.* B **48** 16144
[11] Olijnyk H and Holzapfel W B 1984 *Phys. Lett.* A **100** 191
[12] Ahuja R, Eriksson O, Wills J M and Johansson B 1995 *Phys. Rev. Lett.* **75** 3473
[13] Skriver H L 1982 *Phys. Rev. Lett.* **49** 1768
[14] Jona F and Marcus P M 2006 *J. Phys.: Condens. Matter* **18** 4623
[15] Wentzcovitch R M and Krakauer H 1990 *Phys. Rev.* B **42** 4563
[16] Sofronkov A N, Drozdov V A and Pozhivatenko V V 1992 *Phys. Met. Metallogr.* **74** 140 (Engl. Transl.)
[17] Sliwko V L, Mohn P, Schwarz K and Blaha P 1996 *J. Phys.: Condens. Matter* **8** 799